

# Numerical Investigation Of Hydrodynamics, Liquid Circulation And Mixing In A Lid Driven Cavity

S. Poorvajan<sup>1</sup>, Sv. Sriram Meyapan<sup>1</sup>, R. Rathnakumar<sup>1</sup>

<sup>1</sup>SSN College of Engineering, Chennai, Tamil Nadu (India)

## Abstract

*In this work, we investigate computationally the hydrodynamics and liquid circulation induced by periodic wall in a lid-driven cavity. The system is maintained at adiabatic and isothermal conditions. The top lid is driven periodically such that the plate velocity is proportional to the sinusoidal function of a product of frequency and time. The other three walls are stationary. The Reynolds number for the system is found to be 479. The systematic analysis is carried out by varying the frequency and amplitude of the input velocity on the flow field is investigated. The flow field in a LDC is optimized for the various conditions and best range of frequency would be (0.5-0.9) Hz. The mixing in LDC is investigated by taking an equimolar concentration of acetaldehyde and water. This is quantified using mixing index. Based on the hydrodynamics and mixing studies, it was found that the existence of circulation for good mixing is significant and non-existent for bad mixing.*

problem setup, parallel computing and higher precision. Furthermore, it has all the main features of a complex geometry. The lid-driven cavity problem has long been used a test or validation case for new codes or new solution methods. The problem geometry is simple and two-dimensional, and the boundary conditions are also simple.

The standard case is fluid contained in a square domain with Dirichlet boundary conditions on all sides, with three stationary sides and one moving side (with velocity tangent to the side). The study of the fluid motion in a lid-driven cavity is a classical problem in fluid mechanics. It serves as a benchmark case for understanding complex flows with closed circulation. It also serves as an idealized representation of many industrial process applications such as short-well and flexible blade coaters. With the increasing interest in mixing and chaotic advection, LDC also becomes a model for stirring devices. Two-dimensional (2-D) flow of elastic fluids in a steady lid-driven cavity is studied using Laser Doppler Velocimetry and Particle Image Velocimetry (PIV).

## 1. Introduction

In the past decades, flow in a lid-driven cavity has been studied extensively and it is a well-known bench mark problem for viscous compressible fluid flows. This classical problem has attracted considerable attention because the flow configuration is relevant to a number of industrial applications. The physical configuration consists of a square cavity filled with a liquid. The lid of the cavity moves at a given velocity and translates it, thus setting the fluid in motion. ANSYS FLUENT uses conventional algorithms for calculation of macroscopic variables. Computational advantages of this commercial software are simplicity of the

[3] Reima Iwatsu, Jae Min Hyun and Kunio Kuwahara (1992) performed numerical studies for the flow of a viscous fluid in a two-dimensional square container. The flows were driven by the top sliding wall, executing sinusoidal oscillations. Numerical solutions were acquired by solving the time-dependent, two-dimensional incompressible Navier-Stokes equations. Results were obtained for wide ranges of two principal physical parameters namely Reynolds number and  $\omega$  (non-dimensional frequency of the lid oscillation). They found out that, when  $\omega$  was small, the flow was qualitatively similar to the well-documented steady driven-cavity flow. Flow field obtained by varying frequency of the moving lid showed that the flow in the bulk of cavity region is affected by the

motion of the sliding upper lid. On the contrary, it was deduced that when  $\omega$  was kept large, the fluid motion was confined within a thin layer near the oscillating lid and the flow displayed the characteristic features of a thin-layer flow. When  $\omega$  was kept as an intermediate value, the effect of the side walls was pronounced; the flow pattern revealed significant changes between the low-Re and high-Re limits. The behavior of the force coefficient  $C_f$  were examined from the computational results, characterizations of  $C_f$  as functions of Re and  $\omega$  were attempted. Though flow field was in qualitative consistency with the theoretical predictions, other parameters like amplitude were not considered for analysis.

<sup>[1]</sup>**O'brien (1975)** reported the oscillatory cavity flow which was an extension of his previously studied steady closed rectangular cavity flows (box flows). He added another parameter  $\delta$ , called the height-to length ratio and studied their effect on incompressible laminar flows. Depending on the height-to-length ratio, flow fields were obtained by finite-difference solutions or analytic solutions of the Navier-Stokes equation. He observed an oscillatory parallel flow in the central portion of a flat cavity. Experimental measurements corroborated his theory. Stokes number dependency and particularly differences from the corresponding steady flow (whose Stokes number is zero) were illustrated. The parameter  $\delta$  was a breakthrough in the field of fluid dynamics as it could identify the nature of the fluid within the cavity.

<sup>[2]</sup>**Soh W.H and Goodrich J.W (1988)** presented a new time-accurate finite-difference numerical method for solving incompressible Navier-Stokes equations with primitive variables as the unknowns. The numerical scheme was a Crank-Nicolson implicit treatment of all terms of the equations with central differencing for space derivatives. The lagging of pressure and the nonlinearities in convection terms were corrected by an implicit treatment. Time-accurate solutions were presented for two-dimensional fluid flows in a square cavity with an impulsively starting lid and with an oscillating lid which could easily discretize the cavity with a quicker convergence.

<sup>[6]</sup>**Leong C.W , Ottino J.M ,(1989)** studied the flow field of chaotic mixing in a versatile cavity flow apparatus and conducted a detailed experimental study of mixing in low-Reynolds-number flows. The system was introduced to two

time-periodic co-rotating flows induced by wall motions: one continuous and the other discontinuous. Both types of flows produced exponential growth of circulation within the cavity. The nature of flow was experimentally concluded that a region deep in the cavity also exhibited periodic behavior, similar to the periodically driven cavity. Though the system was complex due the shear stress induced by wall motions, the results obtained indicate that the two-dimensional time-periodic systems can be applied for mixing purposes as proved by the evolution of steady circulations in the flow field.

<sup>[5]</sup>**Pushpavanam et al (2007)** studied the time-dependent fluid flow in a square cavity using model fluids of glycerol-water solution at different frequencies and amplitudes of motion of the top plate. This study was an extension of Reima Iwatsu's earlier predictions of flow field in a lid-driven cavity. The range of Reynolds number was varied from 5 to 3700. Experiments were carried out in a square cavity with a periodically driven lid, and planar velocity measurements were obtained using particle image velocimetry. Temporal variation of velocity at fixed locations in the cavity was found to exhibit a periodic variation. Existence of dominant secondary frequencies observed along the central vertical plane were verified both by experimental and computational studies. The velocity variation as a function of time at a fixed position and the velocity profiles along horizontal and vertical planes were also quantitatively described. Comprehensive details of the flow as a function of Reynolds number were also analyzed. The evolution of secondary vortices at different plate positions as a function of Reynolds number was also presented. At very low Re, the flow throughout the periodically driven cavity qualitatively resembles the classical steady lid-driven cavity flow.

At high Re, the entire cavity is occupied with multiple vortices which matched the predictions of Reima Iwatsu. Though initial studies prove that a lid-driven cavity can be applied for mixing of components of different concentration, they never analyze the efficiency of the mixing studies through parameters like mixing index.

<sup>[7]</sup>**F Javier Martinez Solano et al (2010)** used computational methods for analyzing the concentration fields inside a water storage tank. Computational methods were applied to model flow and concentration field of a tracer within a 3D rectangular water tank. The numerical study

approach based on the Reynolds Averaged Navier-Stokes (RANS) equations was applied to solve closure problem by using the concept of turbulent viscosity. Particularly, the classical two-equation  $k-\epsilon$  model was used. The transport of a tracer inside the tank was also simulated using advection-diffusion equation. Concentration field of each node cell was extracted from the computational data and finally, numerical results demonstrated that about 82% of the tank volume was under complete mixing conditions.

### 1.1 Schematic diagram of a lid driven cavity

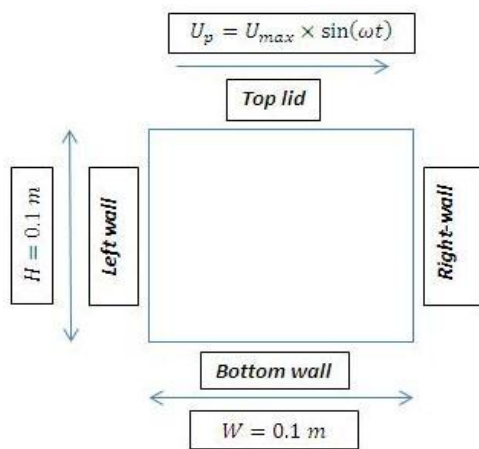


Figure1. Sketch of lid-driven cavity

### 1.2 Applications of lid driven cavity

Lid driven cavity flow studies are useful to improve many practical application prototypes such as short dwell coaters, flexible blade coaters<sup>[2]</sup> and melt-spinning processes in forming continuous metal ribbons. They provide a model for understanding more complex flows with closed recirculation regions, such as flow over a slit, contraction flows and roll coating flows of viscoelastic liquids. In the past, understanding of the recirculating flow within the cavity has been treated as one of the fundamental challenges for fluid dynamics researchers. Therefore, a number of studies have been performed extensively and the solutions for flow behavior are carried out. Most numerical simulations of the driven cavity flow use Navier-Stokes equations.

In recent times, lid-driven cavity finds extensive use in controlled shear tanks, bioreactors for reduced cell disruption and collision of cells is

least desired. Studies have been employed in mixing tanks to prevent agitation (vortex formation) and foaming (a new-age study of mixing tanks without baffles).

## 2. Theory and governing equations

The single phase model equations include the equation of continuity, momentum equation and energy equation (ANSYS Fluent 6.3). The continuity and momentum equations are used to calculate velocity vector. The energy equation is used to calculate temperature distribution and wall heat transfer coefficient. The equation for conservation of mass, or continuity equation, can be written as follows:

### 2.1. Mass conservation equation

The equation for conservation of mass, or continuity equation, can be written as follows:

$$\frac{\partial \rho}{\partial t} + \nabla \cdot (\rho \mathbf{v}) = S_m$$

This equation is the general form of the mass conservation equation, and is valid for both incompressible and compressible flows. A fluid element inside the cavity is thought as the smallest volume for which continuum assumption is valid. Rate of increase of mass in fluid element equals the net rate of flow of mass into the element. It verifies whether the flow per unit area per unit time is conserved for a particular fluid element in the cavity.

### 2.2. Momentum conservation equation

Conservation of momentum in an inertial (non-accelerating) reference frame is described by

$$\frac{\partial \rho}{\partial t} + \nabla \cdot (\rho \mathbf{v} \mathbf{v}) = -\nabla \cdot \mathbf{p} + \nabla \cdot (\boldsymbol{\tau}) + \rho \mathbf{g} + \mathbf{F}$$

Here  $p$  is the static pressure,  $\tau$  is the stress tensor and  $\rho$  and  $\mathbf{F}$  are the gravitational body force, density and external body forces (e.g., that arise from interaction with the dispersed phase) respectively.  $\mathbf{F}$  may also contain other model dependent source terms such as porous-media and user-defined sources. It verifies the rate of change of momentum in the concerned control volume. Here,  $\nabla \cdot (\rho \mathbf{u} \mathbf{u})$  is the convective term which accounts for the velocity field and  $\nabla \cdot \boldsymbol{\tau}$  is the

diffusive term which accounts for the transport due to gradients of shear stress. The stress tensor  $\tau$  is given by:

$$\tau = \mu \left[ (\nabla \cdot \mathbf{v} + \nabla \cdot \mathbf{v}^T) - \frac{2}{3} \nabla \cdot \mathbf{v} \mathbf{I} \right]$$

Here  $\mu$  is the molecular viscosity,  $\mathbf{I}$  is the unit tensor, and the second term on the right hand side is the effect of volume dilation.

### 2.3 Reynolds averaged navier-stokes equation

$$\frac{\partial(\rho u)}{\partial t} + \frac{\partial(\rho u u)}{\partial x} = \rho f + \frac{\partial}{\partial x} \left[ -p\delta + 2\mu \left( \frac{\partial y}{\partial x} \right) - \rho u u \right]$$

The Reynolds averaged Navier-stokes equation verifies the change in mean momentum of fluid element owing to the unsteadiness in the mean flow and the convection by the mean flow. It also helps us to compute the stress term ( $\rho u u$ ) for the given model.

## 3. Computational domain and details about the simulation

### 3.1 Objective

- ❖ To investigate hydrodynamics & liquid circulation in a lid driven cavity.
- ❖ To investigate mixing of two miscible liquid having different concentration.

### 3.2 Problem description

- ❖ Investigation of hydrodynamics and mixing in a 2-D lid driven cavity of size (0.1m×0.1m).
- ❖ The vertical lids are kept under adiabatic and isothermal conditions.
- ❖ The top lid is moved periodically (i.e. plate velocity is proportional to the sinusoidal function of product of time and frequency).

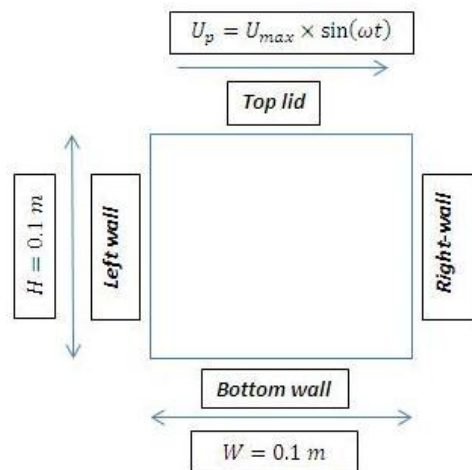


Figure 2. Computational Domain of the lid-driven cavity.

### 3.3 Assumptions

- The flow field in within the cavity is two-dimensional and unsteady state.
- To investigate the hydrodynamics, water is being used.
- The two-dimensional system is maintained under adiabatic conditions such that no heat loss through the side walls of the cavity is considered.
- The model is single phase without accounting for the multiphase interactions.

### 3.4 Boundary conditions

- Vertical lids maintained under adiabatic and isothermal conditions
- Top lid velocity is defined as:

$$U_p = U_{max} * \sin(\omega t)$$

Where,  $U_{max} = A * \omega$  is the maximum plate velocity (m/s). Here,  $A$  is the amplitude and  $\omega$  is the angular frequency.

- The other faces of the cavity are considered as solid stationary walls.
- The gravity acts in negative Y-direction.
- No slip at the sides of solid walls.

### 3.5 Simulation methodology

- The CFD simulations were performed using Fluent 6.2 software. The 2-D Quad-map grid is obtained using Gambit 2.1.
- A periodic boundary condition is defined by an external user defined function which is later interpreted into Fluent for hydrodynamic studies.
- Simulations were performed in an unsteady state system and iterations were performed till a period 50 s with a time step size of 0.01 s.

### 3.6 Meshing of the geometry

Structured meshing method done in GAMBIT 2.1 was used for meshing the geometry. 100×100 node cells were created using a Quad scheme. Boundary conditions are also defined after meshing the geometry.

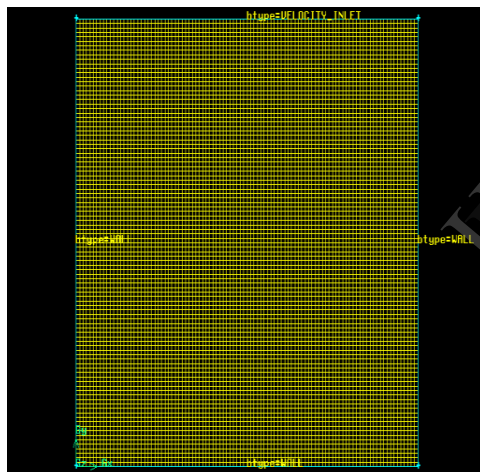


Figure 4. Meshed geometry of a lid-driven cavity

## 4. Results and discussions

### 4.1 Effect of mesh size on flow field

The computational studies were carried out for different mesh sizes namely 0.5, 0.1 and 0.01. The flow fields were plotted at the end of 50 seconds.

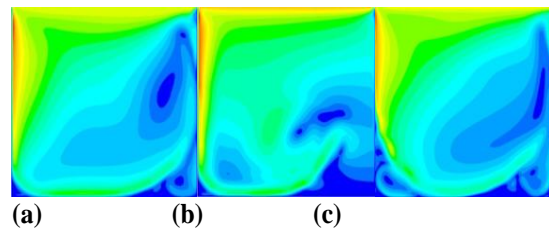


Figure 3.(a) Contour plot for the mesh size 0.01, (b) Contour plot for the mesh size 0.1, (c) Contour plot for the mesh size 0.5.

To investigate quantitatively, components of velocity magnitude are analyzed for various the mesh sizes such as 0.01, 0.1 and 0.05 with 10210 node cells in order to deduce the optimum mesh size for carrying out the studies.

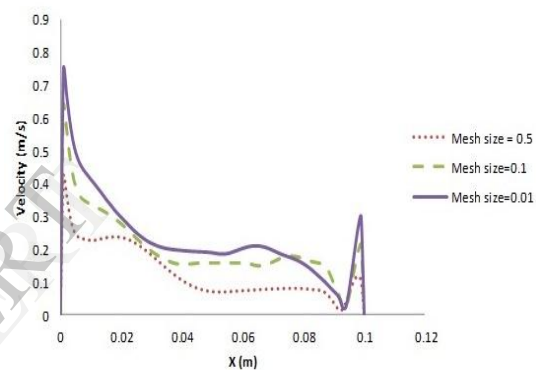


Figure 5. Variation of velocity magnitude with mesh size

It was observed from figure 5 that there is no significant effect of mesh size on flow field as liquid circulation exists in all the considered mesh sizes. Since a mesh size of 0.01 consists of more node cells, the contribution of each node cell gives a more detailed and accurate analysis of the flow field. The details of the optimized grid are mentioned below.

### Details of the Grid used for the cavity

Level	Cells	Faces	Nodes	Partitions
0	10000	20200	10201	1

1 cell zone, 3 face zones, grid size: 100\*100.



## 4.2 Effect of time step on flow field

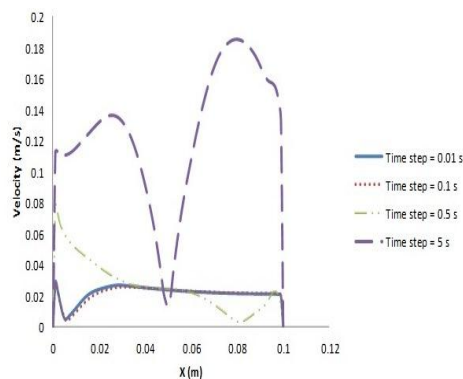


**Figure 6.** Variation of velocity magnitude with time step.

To find the optimum time step, variation of components of velocity along the HZ line is analyzed for various time steps such as 0.01s, 0.1s, 0.5s and 5s. From figure 6, it is found that at increasing time step values, evolution of stable circulations within the cavity decreases. It is observed that there is no significant change in the components of velocity when the time step is 0.01s. For optimizing time step for further studies, this region of constant velocity magnitude indicating a steady state occurrence after a time period of 50 s is considered. Since there are greater fluctuations of magnitude of velocity within the cavity for higher time step values, such values are ignored due to the unsteady nature of flow field profiles.

## 4.3 Variation of amplitude with flow field

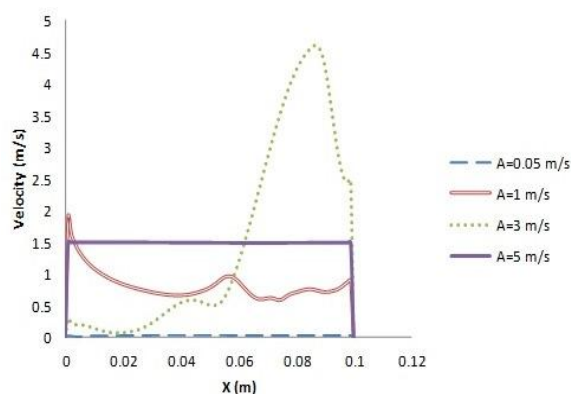
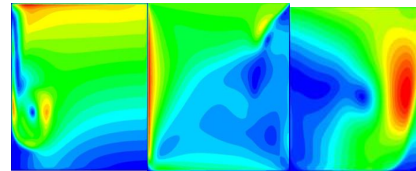


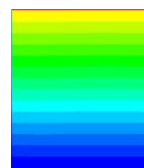
**Figure 8.** Variation of velocity magnitude with Amplitude.

The parameter amplitude of the moving lid is varied and its effect on flow field is studied. It was

found that with increase in the amplitude of the lid, the evolution of circulations within the cavity decreases. When there is an increase in amplitude of the lid, fluctuations of velocity within the cavity becomes predominant. A no flow-field condition was deduced which indicates the negligible effect of the moving lid of the flow field. The plot shows that a no field condition at  $A=5$  m/s.



(a) (b) (c)



(d)

**Figure 7.** Variation of contours of Velocity magnitude with amplitudes, a)  $A=0.05$  m/s, b)  $A=1$  m/s, c)  $A=3$  m/s, d)  $A=5$  m/s.

From the above contour plots it is evident that the amount of circulation decreases with the increase in with no stagnant regions in case of lower amplitudes. Hence the amplitude of 0.05m/s was assumed to be the most efficient one as any decrease in amplitude will result in an insignificant circulation. On varying the amplitude for the system, it was found that at lower amplitudes, the effect of periodic motion is able to penetrate the subsequent layers of the fluid and result in the evolution of vortices. But, at higher amplitudes, this effect is nullified and no circulations are observed rendering the system incapable for performing mixing and hydrodynamic studies if multiple components are used in the cavity.

#### 4.4 Variation of frequency on the flow field

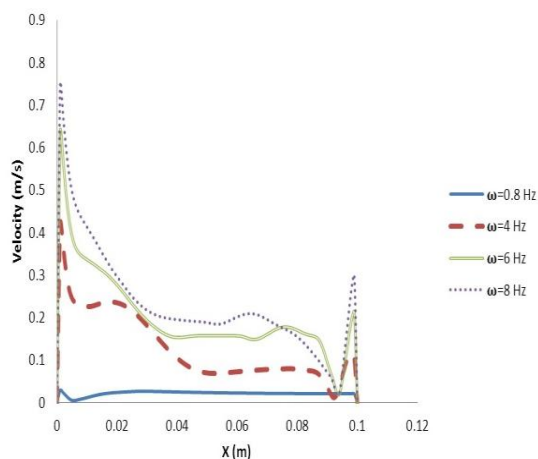
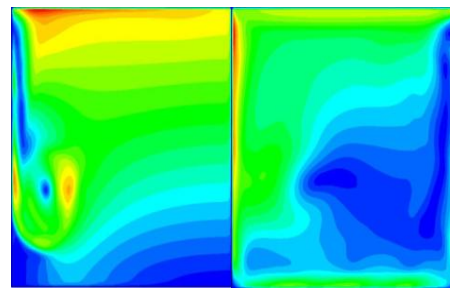


**Figure 9.** Variation of velocity magnitude with frequency along the HZ line.

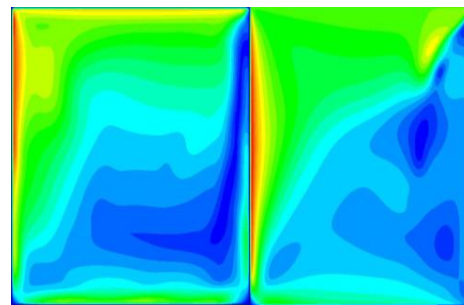
The parameter angular frequency of the moving lid is varied and its effect on the flow field is studied. Studies were further carried out for different frequencies and the velocity plots were drawn and compared. The velocity magnitude corresponding to  $Y=0.05$  meters was plotted and compared for various frequencies.

It is observed that the circulations present in the flow field decreases with an increase in frequency. When frequency of the moving lid is increased, the convergence criterion is affected as the system encounters a greater fluctuation of velocity within the cavity which results in a longer flow time to attain a steady flow field. Moreover, when the frequency is low then the shear stress induced by the moving lid penetrates deeper and its effect is predominant as a steady flow field is attained at a lesser flow time. Thus, considering this criteria  $\omega=0.8$  Hz is taken as the optimum value of frequency for hydrodynamic studies.

From the contour plots it is shown that the steady flow field is obtained for  $\omega=0.8$  Hz thus qualitatively proving the graphical data.



(a) (b)



(c)(d)

**Figure 10.** Variation of contours of VM with frequencies, a)  $\omega=0.8$  H , b)  $\omega=4$  Hz, c)  $\omega=6$  Hz, d)  $\omega=8$  Hz.

#### 4.5 Variation of components of velocity with depth of the cavity

The Hydrodynamic behavior of the lid-driven cavity can be studied in terms of velocity distribution within the cavity. The numerical value of  $Re$  was found to be 479 for the lid moving periodically with an amplitude of 0.05 m/s and a frequency of 0.8 Hz. The variation of components of velocity along the width of the cavity for water are displayed in figure 10. The figure shows that for an incompressible fluid (water), the magnitude of components of velocity is maximum near the region of fluid adjacent to the periodically moving lid. When there is a shift of region to a higher height within the cavity, the magnitude of both the components of velocity increases.

Thus was found that magnitude of both components of velocity are maximum near the region adjacent to the periodically moving lid, (i.e.)  $H=0.08$  meters.

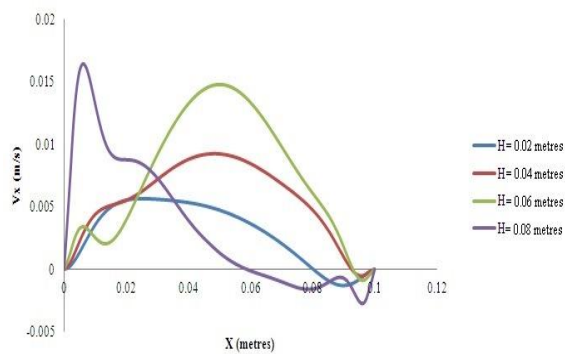


**Figure 11.** Variation of X-component velocity along HZ line.

The following table illustrates numerical values of X-velocity at a fixed width of the cavity  $X=0.05$  metres.

**Table1.**  $V_x$  at fixed width  $X=0.05$  m.

Position (height) (m)	0.02	0.04	0.06	0.08
$V_x$ (m/s)	0.004741	0.009238	0.014798	0.001324

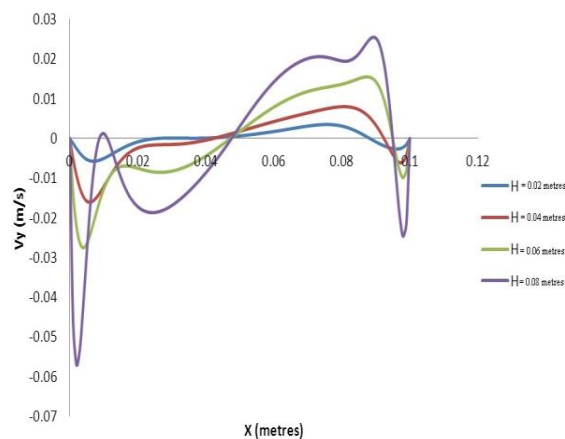


**Figure 12.** Variation of Y-component velocity along HZ line.

The following table illustrates numerical values of Y-velocity at a fixed width of the cavity  $X=0.05$  metres.

**Table2.**  $V_y$  at fixed width,  $X=0.05$  m.

Position (height) (m)	0.02	0.04	0.06	0.08
$V_y$ (m/s)	0.000637	0.001793	0.001769	0.003011

#### 4.6 Variation of components of velocity with curve- length

Four different regions with increasing height were chosen within the cavity and studies confirmed that the magnitude of velocity is maximum near the region adjacent to the periodically driven cavity. The variations of velocity at  $Re=479$  and  $Pr=5.53$  are shown below. The X-component velocity shows a decrease in velocity at the region adjacent to the lid, but the increase in Y-component velocity is sufficient to compensate the decrease in the magnitude of X-component to prove that the resultant magnitude of velocity vector ( $V_{mag}$ ) increases with increase in a region of increasing height within the cavity.

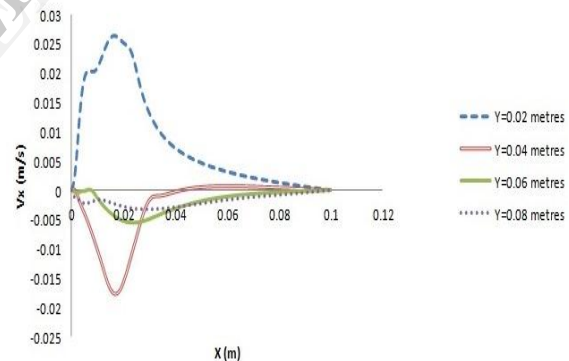


**Figure 13.** Variation of  $V_x$  with  $X$  (m).



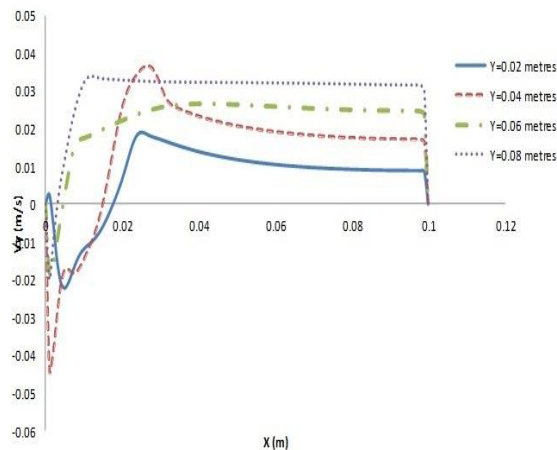


Figure 14. Variation of  $V_y$  with  $X$  (m).

#### 4.7 Variation of flow field with time

Based on the optimized time step and mesh size and other parameters that affect the flow field within the lid-driven cavity, contour plots were generated that specifies the magnitude of velocity at each node cell which is used of analysis of the flow field.

##### 4.7.1 Variation of velocity magnitude contours

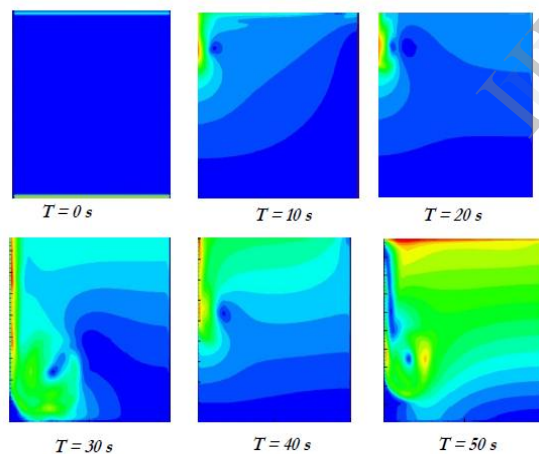


Figure 15. Variation of flow field with time

A Contour plot gives the numerical value of velocity magnitude of each node cell within the lid-driven cavity. As the time progresses, there is a significant change in the magnitude of velocity from flow time  $T=0$  to  $T=50$  s. The change in the magnitude of velocity is attributed to the motion of the top lid.

##### 4.7.2 Variation of stream lines with time

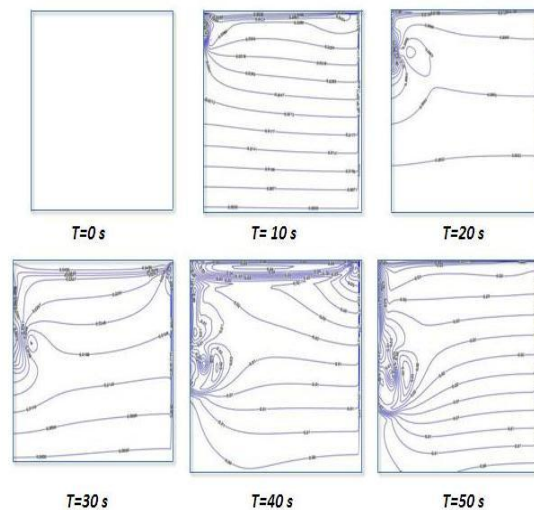
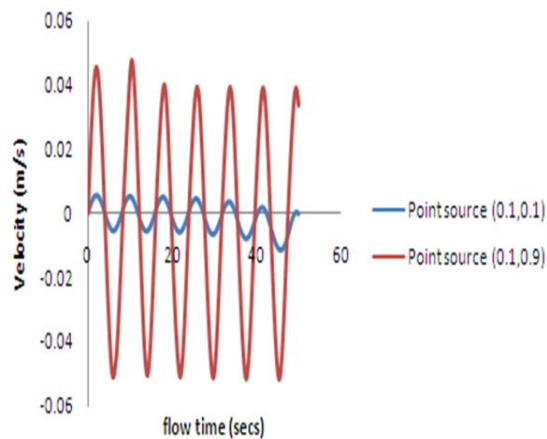


Figure 16. Variation of liquid circulation with time.

The streamline plot gives numerical value of stream function for each node cell within the lid-driven cavity. Here it is observed that as the time progresses, there is a significant distribution of velocity field throughout the cavity till a flow time of 50 s. Beyond this flow time, the system attains steady state and there is no considerable change in flow field.

#### 4.8 Temporal variation of flow field

- It was speculated that since the nature of plate velocity or the velocity of the moving lid in the cavity is sinusoidal, any region within the cavity should show periodic nature due to the effect of the moving lid.
- Two point sources namely, (0.1,0.1) and (0.1,0.9) were considered in the present investigation. The variation of velocity magnitude with flowtime for these point sources is calculated and shown in figure 16.



**Figure 17.** Temporal variation of velocity magnitude at point sources.

The point (0.1,0.1) is located near the top lid and the point (0.1,0.9) is located near the bottom wall. It is observed that a sinusoidal variation exists in these regions due to the penetrating effect of motion of the lid. The sinusoidal variation indicates that, irrespective of the position of the point source in the cavity the variation is sinusoidal, though the magnitude depends on the location of the point in the cavity.

#### 4.9 Power spectrum analysis

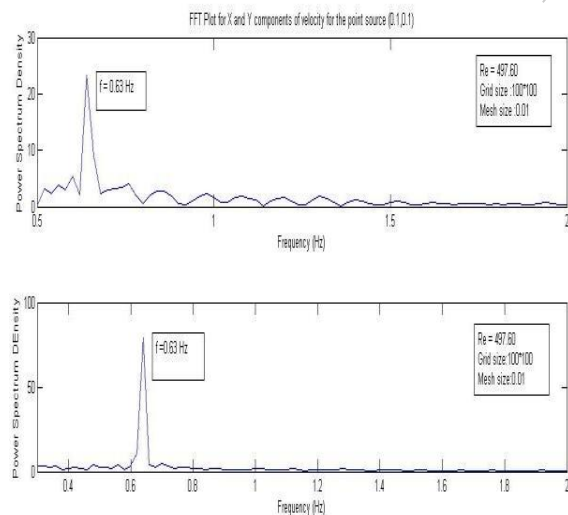


**Figure 18.** Power Spectrum Analysis.

The effect of the periodic motion of the lid on the fluid and the nature of flow within the system can

be assessed by generating frequency plots that determine whether the flow is turbulent or laminar at that particular point source. The power spectrum analysis for a component of velocity generates a single peak which shows that the nature of flow inside the cavity is laminar. If multiple peaks are generated in the FFT plots, it indicates turbulence within the system at the particular selected point source. If a single dominant peak is observed, then laminar nature of the fluid is confirmed. It was found that the dominant frequency for these points were quite similar to the operating frequency of the periodically moving cavity.

#### 4.10 Mixing studies

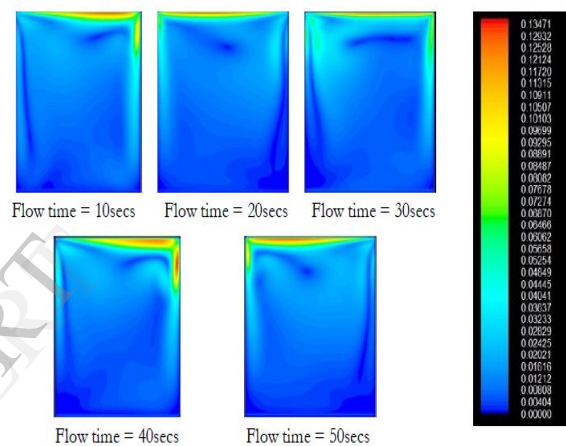
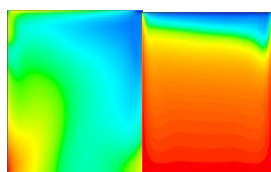


**Figure 19.** Contour plots indicating existence of flow field within the cavity at a)  $t=10$  s, b)  $t=20$  s, c)  $t=30$  s, d)  $t=40$  s, e)  $t=50$  s.

The optimized values of the parameters used in hydrodynamic studies were employed for analyzing the flow field obtained for mixing studies. Two components of same composition namely acetaldehyde (50%) and water (50%) were taken as materials inside the cavity. Efficiency of mixing is found out using numerical values of mixing indices for each time period of 10 s. It was found out that the flow fields obtained for mixing studies were similar to the flow fields obtained for hydrodynamic studies indicating a steady flow field due to uniform mixing.

#### 4.11 Contour plots for other parameters



(a)

(b)

**Figure 20.** Contour plots showing magnitude of  
a)Temperature, b) Molar concentration of  
acetaldehyde.

<i>X (m)</i>	<i>Y(m)</i>	<i>Concentration of acetaldehyde (kmol/m<sup>3</sup>)</i>
4.50E-02	9.00E-02	6.40E-03
4.60E-02	9.00E-02	6.46E-03
4.70E-02	9.00E-02	6.52E-03
4.80E-02	9.00E-02	6.58E-03
4.90E-02	9.00E-02	6.63E-03
5.00E-02	9.00E-02	6.69E-03
5.10E-02	9.00E-02	6.75E-03
5.20E-02	9.00E-02	6.81E-03
5.30E-02	9.00E-02	6.86E-03

#### 4.12 Mixing index

To obtain the efficiency of mixing within the cavity, concentration of the resultant mixture from each node cell were extracted after each flow time of 10 s. Using the numerical values of these concentration fields, mixing index was calculated for each time period. Mixing index is later formulated with these values of concentration fields. A comparison study is later made with the mixing indices and the trend of mixing indices is found out for each flow time. The concentration field of each node cell is discretized using SIMPLE algorithm. The following tabular column shows the numerical values of concentration fields for a flow time of 50 s.

**Table 3.** Sample values of discretized  
concentration field of each node cell

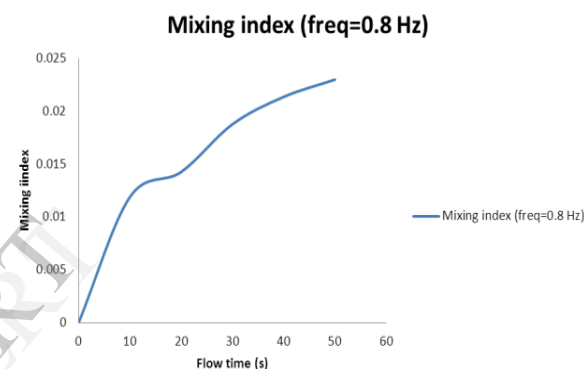


**Figure 21.** Variation of Mixing index with Flow  
time

It was found out mixing index shows an increasing trend with respect to flow time. As time progresses a more uniform flow field with steady circulations. The mixing studies were carried at amplitude and frequency of 0.05 m/s and 0.8 Hz respectively.

**Table 4.** Sample values of mixing index with the  
corresponding flow time

<i>Flow time (s)</i>	<i>Mixing index</i>
0	0
10	0.01189
20	0.01458
30	0.018775
40	0.021366
50	0.023

#### 4.13 Variation of temperature along depth of the cavity

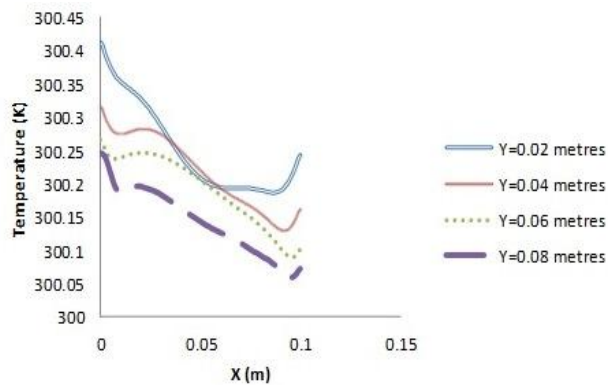


**Figure 22.** Variation of Temperature with depth of the cavity

The variation of temperature along various levels in the cavity, the temperature profiles is analyzed and is shown in figure 21. It is observed that the temperature of the mixture within the cavity decreases as the depth of the cavity increases. This is due to increase in enthalpy of mixing as the time progresses which confirms uniform mixing in the lower regions of the cavity.

## 5. Conclusion

The hydrodynamics and mixing are investigated in a lid driven cavity using CFD. The investigations are carried by varying frequency, time step and amplitude of the moving lid to obtain the flow field in a LDC. It was found that the flow field obtained from the hydrodynamic studies and mixing studies have a similar profile due to the evolution steady circulations. The temporal variation of velocity magnitude at a point source is considered for the investigation and it was found the sinusoidal variation of velocity magnitude at the point was due to the periodic motion of the lid.

The range of frequency at which the best circulations are observed in a flow field is calculated and is found to be 0.5-0.9 Hz. At low level of amplitude and frequency of the lid, it was found that higher penetration effect on the flow field within the cavity. Finally, the parameters affecting the flow field within the cavity is optimized. To investigate the mixing, equimolar concentration of reactants are considered. The mixing in LDC was quantified by mixing indices. It was found that the mixing is uniform as the time progresses and uniform concentration of the mixture was observed at the end of 50 s.

## 6. References

- [1] O'Brien V., 1975, "Unsteady cavity Flows: Oscillatory Flat Box Flows" *Journal of Applied Mechanics*, Transactions of ASME, 557-563.
- [2] Soh W. H., and Goodrich, J. W., 1988, "Unsteady Solution of Incompressible Navier-Stokes Equations," *Journal of Computational Physics*, 79, 113-134.
- [3] Iwatsu, R., Hyun, J.M. and Kuwahara, K., 1992, "Numerical Simulations of flows driven by a Torsionally Oscillating Lid in a Square Cavity," *Journal of Fluids Engineering*, 114, 143-151.
- [4] Iwatsu, R., Hyun, J.M. and Kuwahara, K., 1993, "Numerical Simulations of Three Dimensional Flows in a Cubic Cavity with an Oscillating Lid," *Journal of Fluids Engineering*, 115, 680-686.
- [5] Sriram, S., Deshpande A. P., and Pushpavanam S., 2006, "Analysis of spatiotemporal variations and flow structures in a periodically-driven flow," *Journal of Fluids Engineering*, 128, 413- 420.
- [6] Leong C. W., Ottino J. M., 1989, "Experiments on mixing due to chaotic advection in a cavity," *Journal of Fluid Mechanics*, 209, 463-499.
- [7] F. Javier Martínez-Solano, Pedro L. Iglesias Rey, Carlo Gualtieri, P. Amparo López-Jiménez, 2010 "Modeling flow and concentration field in rectangular water tanks ", *Journal of International Congress on Environmental Modeling and Software*, 289, 403-409.